Original Article

OPEN

Association of central arterial stiffness with hippocampal blood flow and *N*-acetyl aspartate concentration in hypertensive adult Dahl salt sensitive rats

Samuel O. Ajamu[a], Rachel C. Fenner[a], Yulia N. Grigorova[a], Defne Cezayirli[a], Christopher H. Morrell[a], Edward G. Lakatta[a], Mustapha Bouhrara[b], Richard G. Spencer[b], Olga V. Fedorova[a,*], and Kenneth W. Fishbein[b,*]

Background: Central arterial stiffness (CAS) is associated with elevated arterial blood pressure (BP) and is likely associated with stiffening of cerebral artery walls, with attendant cerebral hypoperfusion, neuronal density loss and cognitive decline. Dahl salt-sensitive (Dahl-S) rats exhibit age-associated hypertension and memory loss, even on a normal salt intake.

Method: We sought to explore whether central arterial pulse wave velocity (PWV), a marker of CAS, is associated with hippocampal cerebral blood flow (CBF) and neuronal density in hypertensive Dahl-S rats. We measured systolic BP (by tail-cuff plethysmography), aortic PWV (by echocardiography) and CBF and *N*-acetyl aspartate (NAA) (by magnetic resonance imaging) in 6 month-old male Dahl-S rats ($n = 12$).

Results: Greater PWV was significantly associated with lower CBF and lower NAA concentration in the hippocampus, supporting a role of CAS in cerebrovascular dysfunction and decline in cognitive performance with aging.

Conclusion: These findings implicate increased CAS in cerebral hypoperfusion and loss of neuronal density and function in the Dahl-S model of age-associated cardiovascular dysfunction.

Keywords: aging, arterial blood pressure, arterial stiffness, brain metabolites, cerebral blood flow, Dahl salt-sensitive rats, hippocampus, hypertension, magnetic resonance imaging, *N*-acetyl aspartate, neuronal density, pulse wave velocity

Abbreviations: aPWV, aortic pulse wave velocity; ASL, arterial spin labeling; BP, blood pressure; CAS, central arterial stiffness; CASL, continuous arterial spin labeling; CBF, cerebral blood flow; Dahl-S, Dahl salt-sensitive; ECG, electrocardiogram; FDR, false discovery rate; HR, heart rate; MRI, magnetic resonance imaging; MRS, magnetic resonance spectroscopy; NAA, *N*-acetyl aspartate; PLD, post-labeling delay; PWV, pulse wave velocity; ROI, region of interest; SBP, systolic blood pressure; SD, standard deviation; SNR, signal to noise ratio; tCr, total creatine

INTRODUCTION

Aging is a major risk factor for cardiovascular disorders and dementia. The global burden of dementia is projected to increase by 50% over the next decade. Further elucidation of the underlying pathophysiology will be required for the development of effective therapeutics. For over two decades, epidemiological and clinical studies have shown strong associations between vascular risk factors and dementia [1–5], indicating that diseases of the vascular wall, that is, stiffening of the arterial wall and hypertension, may be significant contributors to vascular dementia [6–11]. Untreated hypertension stage I is characterized by systolic blood pressure (SBP) in the range of 130–139 mmHg, and hypertension stage II is diagnosed when SBP is ≥140 mmHg, as determined by the American Heart Association (AHA) Guideline (https://www.heart.org/en/health-topics/high-blood-pressure). However, the mechanisms linking vascular stiffening with dementia are not fully understood.

In normal cardiovascular physiology, at the end of ventricular ejection, the pressure in the aorta falls much more slowly than in the left ventricle. This is because the large central arteries, including the aorta, are elastic and thus act as a reservoir during systole, storing some of the ejected blood. This blood is then forced into the peripheral vessels during diastole through the Windkessel effect [12].

Journal of Hypertension 2021, 39:2113–2121

[a]Laboratory of Cardiovascular Science and [b]Laboratory of Clinical Investigation, Magnetic Resonance Imaging and Spectroscopy Section, National Institute on Aging, National Institutes of Health, Baltimore, Maryland, United States

Correspondence to Kenneth W. Fishbein, 251 Bayview Blvd, Baltimore, MD 21224, USA. E-mail: fishbeink@mail.nih.gov

*Drs Olga V. Fedorova and Kenneth W. Fishbein contributed equally to this work.

Written work prepared by employees of the Federal Government as part of their official duties is, under the U.S. Copyright Act, a ''work of the United States Government'' for which copyright protection under Title 17 of the United States Code is not available. As such, copyright does not extend to the contributions of employees of the Federal Government.

Received 22 September 2020 **Revised** 22 April 2021 **Accepted** 26 April 2021

J Hypertens 39:2113–2121

DOI:10.1097/HJH.0000000000002899

Some kinetic energy is stored as potential energy in the elastic conduit arteries during systole. With increased central arterial stiffness (CAS), less potential energy is stored during systole, which results in impaired, pulsatile and erratic flow during diastole [12,13], that is, CAS decreases the Windkessel phenomenon and increases reflected waves leading to increased systolic and decreased diastolic pressure. Increased CAS induces a decrease of the compliance of the central arteries, not only due to an increase in collagen abundance [14–16], but also due to elastin fragmentation within central arterial walls, resulting in a reduction in the elastin-to-collagen ratio [10,17,18]. CAS increases with aging [19,20], and is often accompanied by an increase in blood pressure (BP).

Methods of measuring arterial stiffness vary depending on the location of focus: local, regional or systemic. Pulse wave velocity (PWV) estimation is a method that provides a regional measure of stiffness [21]. The velocity of blood through a specific vessel segment is inversely proportional to the distensibility of the vessel. Specifically, measuring the velocity of a pulse wave from the transverse aorta to the abdominal aorta provides an index of CAS [22,23]. This metric as well as other hemodynamic parameters become important when trying to understand the role vascular effects play in peripheral organs such as the brain.

Circulating blood supplies the brain with oxygen and nutrition and removes the products of cell metabolism. In humans, the brain comprises only 2% of the body's weight but sequesters about 15% of the cardiac blood output. Additionally, in a ratio disproportional to its weight, the brain consumes about 20% of the total body's oxygen demand [24]. Understanding how CAS affects cerebral circulation and perfusion could provide insights into the mechanism of cognitive decline and dementia. One component that links CAS with cerebral composition and function is cerebral blood flow (CBF). CBF can be measured using magnetic resonance imaging (MRI) with arterial spin labeling (ASL). This utilizes magnetic tagging of water protons in blood to quantify the amount flowing through a specific imaging slice. From this, mean CBF values can be measured in regions of interest within the given slice. Lower CBF has been correlated with greater pulsatility and stiffness, as assessed by carotid to femoral PWV [25–27]. One mechanism proposes that an impedance mismatch between the aorta and carotid arteries results in pulse wave reflection, which normally provides a protective hemodynamic buffer to prevent excessive pulsatile flow from reaching the brain. With CAS, proximal aortic stiffening increases aortic impedance, thereby decreasing this impedance mismatch and allowing transmission of excessive pressure and flow pulsatility into the cerebral circulation. These abnormal physical forces trigger vascular damage and remodeling that limits flow, presumably leading to microvascular ischemia, quantifiable tissue damage and reduced cognitive performance [10,11,25,26].

N-acetyl aspartate (NAA) is a neuronal marker found abundantly in the central nervous system [28]. One means of detecting neuronal loss is through the measurement of NAA concentration. The concentration of NAA can be measured by localized magnetic resonance spectroscopy (MRS) and is frequently cited as a metric of neuron health and viability. A reduced NAA concentration is indicative of mitochondrial dysfunction and neuronal loss [29]. In general, NAA concentration, whether measured as an absolute concentration or as a ratio to total creatine (tCr), is diminished in neurodegenerative disorders [30,31]. In primary degenerative dementia, for which definitive diagnosis depends on neuropathological examination, the NAA/tCr ratio was significantly lower than in healthy age-matched controls. This effect was observed even in dementia patients with no significant deficit in regional cerebral blood flow or brain atrophy. Additionally, other works have shown evidence of deficits in NAA within ischemic brain regions [32].

Here, we studied Dahl salt sensitive (Dahl-S) rats [33,34], which exhibit CAS and hippocampal spatial memory decline as they develop a variable degree of moderate hypertension with age (average SBP 150–160 mmHg in 6 month-old Dahl-S rats) [33,34], comparable to the presentation of hypertension stage II in humans. We employed the Dahl-S rat model of age-associated hypertension and CAS to elucidate links between arterial stiffening in the systemic circulation and deficits in cerebral perfusion and neuronal density in the hippocampus. We hypothesized that higher aortic PWV, a marker of CAS, is associated with lower hippocampal CBF and neuronal density in adult Dahl-S rats maintained on a normal salt intake.

METHODS

Experimental design

The study design was approved by the local Animal Care and Use Committee (Intramural Research Program, National Institute on Aging, National Institutes of Health) and all procedures were performed in accordance with institutional guidelines. Twelve male Dahl-S rats (SS/JrHsd, Charles River Laboratories, Frederick, MD) were maintained on a normal salt diet (0.5% NaCl) (Harlan Teklad, Madison, WI) and tap water ad libitum for the duration of the study. The rats were housed pairwise in plastic cages at 25°C with a 12 h light/12 h dark cycle. All physiological and MRI measurements were acquired at 6 months of age and over a time frame of no more than 2 weeks.

SBP was recorded by tail-cuff plethysmography (IITC Inc, Woodland Hills, CA) in conscious rats. For this measurement, the animals require handling, warming and restraint in order to obtain reliable results [35]. The rats were habituated to restraint in a plastic tube with a tail cuff at 32°C for a minimum of 30 min/day over 2 days prior to measurement. After 5 min of acclimation, five consecutive measurements were performed with a 1 min interval between repetitions. The set of five consecutive measurements was repeated, if necessary, in order to obtain a stable reading. Finally, the average of the five stable readings was recorded [34].

Aortic PWV (aPWV) was measured in rats sedated with 2.5% isoflurane in oxygen for restraint. The animals were maintained on a heating pad in the supine position. The chest was shaved, electrocardiogram (ECG) leads were placed on two front legs and one rear leg, and an ECG tracing was recorded. Aortic PWV was measured by the transit time method using a Vevo 3100 system

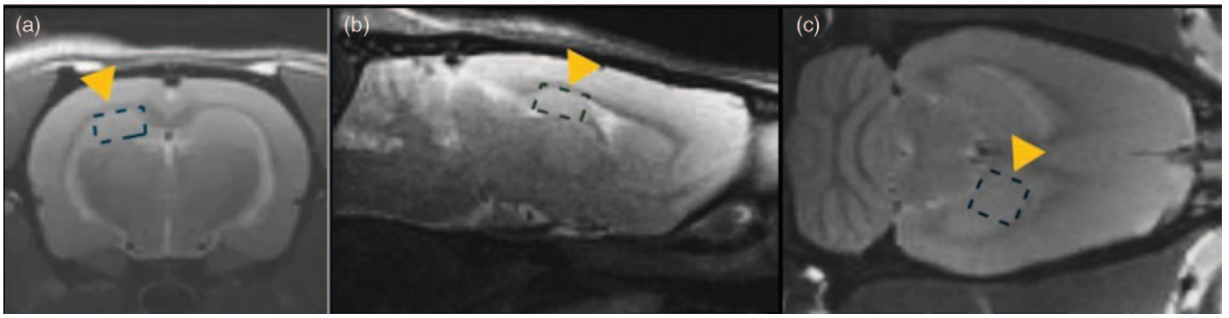

FIGURE 1 Voxel Placement for 1H Spectroscopy of the Right Hippocampus. Representative in-vivo T_2-weighted MR images of a Dahl-S rat brain. (a) Coronal, (b) sagittal and (c) axial brain slices with yellow arrowhead indicating a dashed region of interest (ROI), placed in the right hippocampus, where localized proton NMR spectra were acquired.

(VisualSonics, Toronto, Canada) with a MX250S transducer at the transverse aortic arch and the abdominal aorta [36]. The time at the transverse aortic arch (t_1) and at the abdominal aorta (t_2) were defined as the time from the peak of the ECG P wave to the foot of the velocity upstroke. The transit time (ΔT) of the flow wave from the upper thoracic aorta to the lower abdominal aorta was determined as the difference between the two measurements ($t_2 - t_1$). The distance between these two locations (D) was measured and aPWV was calculated as $D/\Delta T$. Each measurement of aPWV in each animal represents the average of five independent recordings. Representative Doppler images that were used for aPWV measurements are presented in Figure S1, Supplemental Digital Content, http://links.lww.com/HJH/B666, and the individual measurements for t_1, t_2 and D are presented in Table S3, Supplemental Digital Content, http://links.lww.com/HJH/B666.

Brain NAA concentration was measured in the right hippocampus using a 7T Bruker Biospec MRI scanner (Billerica, MA). Rats were sedated with 2% isoflurane in oxygen and placed prone in a custom animal bed (RAPID MRI International, Columbus, OH). Vital signs were monitored throughout the MRI examination (SA Instruments, Stony Brook, NY). Respiration rate was maintained at 45–55 min^{-1} by small variations in the inhalation mixture. For data acquisition, a $2.5\,mm \times 1.5\,mm \times 2.5\,mm$ spectroscopic voxel was placed in the right hippocampus (Fig. 1), and a spectrum was measured using a PRESS sequence with CHESS water suppression, echo time $TE = 15.7\,ms$, repetition time $TR = 2.5\,s$, spectral width $= 6010\,Hz$ and 128 averages. NAA concentration, calculated using the unsuppressed water peak as a reference, and the ratio of NAA to tCr were calculated using LCModel, a software package that calculates metabolite concentrations from ^1H NMR spectra [37]. Localized shimming centered on the hippocampus was implemented, with resulting water linewidths within the 7–10 Hz range.

CBF was measured using continuous arterial spin labeling (CASL) in the coronal slice with the largest hippocampal area (Fig. 2). Data were acquired using an echo planar

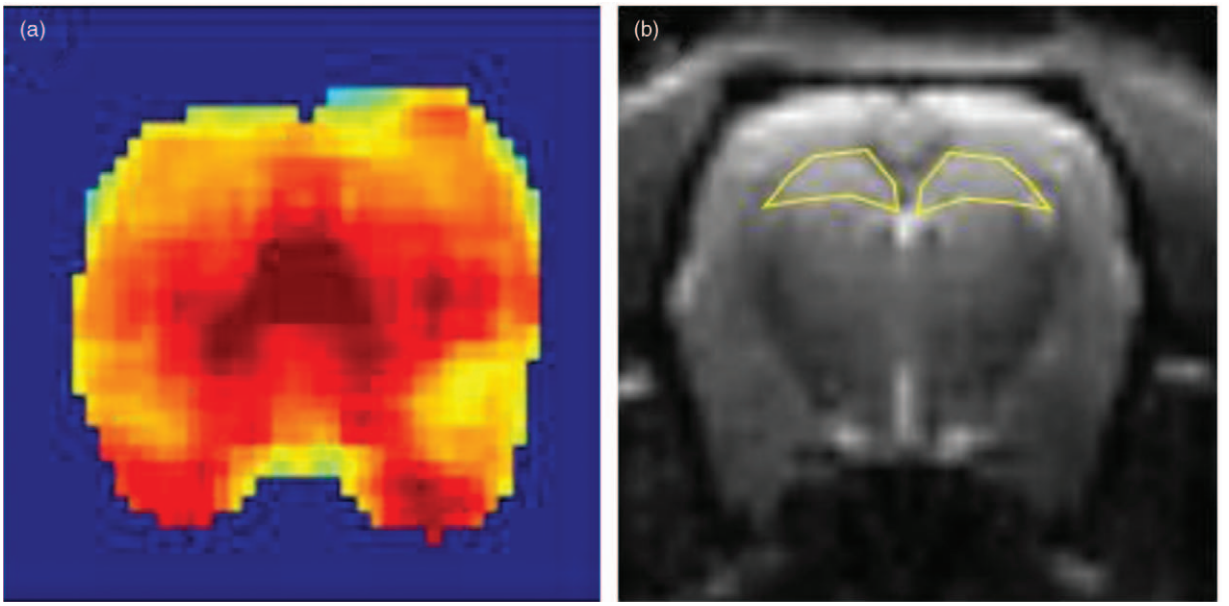

FIGURE 2 Representative CBF Map and ROI Placement for Measurement of Hippocampal Perfusion in the Dahl-S rat brain. (a) Coronal CBF map calculated from filtered CASL images. (b) Proton density-weighted image showing a region of interest (ROI) for calculation of hippocampal CBF. For CBF measurement, slice position was chosen to maximize the cross-sectional area of the hippocampus (yellow lines). CASL, continuous arterial spin labeling; CBF, cerebral blood flow; Dahl-S, Dahl salt-sensitive.

imaging sequence with echo time TE = 28 ms, repetition time TR = 5 s, 64 × 64 pixels, 0.469 mm × 0.469 mm × 1 mm voxel size, labeling duration $\tau = 2$ s and postlabeling delay (PLD) = 0.1 s. There were 5 repetitions of one contralateral (control) and one labeling scan. An experiment with no labeling was additionally conducted with 5 repetitions. The nonlocal estimation of multispectral magnitudes (NESMA) filter [38] was applied to the averaged images and a region of interest (ROI) spanning both the right and left hippocampus was manually defined with reference to a corresponding proton density-weighted image (Fig. 2b). Some individual representative CBF images and numerical data are presented in Figures S2–S5, Supplemental Digital Content, http://links.lww.com/HJH/B666 and in Table S4, Supplemental Digital Content, http://links.lww.com/HJH/B666. Mean CBF was calculated using a standard model, assuming values for the brain/blood partition coefficient $\lambda = 0.9$ ml/g, labeling efficiency $\alpha = 0.85$ and $T_{1,blood} = 2300$ ms [39,40] (Fig. 2a).

Statistical analysis

All statistical analyses were performed with R software (Open Source). Shapiro-Wilk normality tests were conducted for each variable. All samples passed the normality test ($P >> 0.05$), showing that each variable has a Gaussian distribution. Results are reported as mean ± standard deviation (SD). Next, a linear regression analysis was performed to obtain the coefficients of the regression line and corresponding *P*-values (RStudio). A two-tailed *P*-value less than 0.05 was considered significant. A symmetric correlation matrix of all parameters was calculated using R. The correlations were adjusted for false discovery rate (FDR). In addition, multiple regression analysis was conducted to investigate the relationship between NAA, CBF and other variables.

TABLE 1. Physiological and MRI parameters in 6 month-old male Dahl-S rats

Parameters	*n* = 12
Body weight (g)	439 ± 24
Systolic blood pressure, SBP (mmHg)	162 ± 13
HR during SBP measurement (in conscious rats) (beats/min)	418 ± 23
Aortic pulse wave velocity (m/s)	5.25 ± 0.92
HR during PWV measurement (in anesthetized rats) (beats/min)	340 ± 25
Hippocampal blood flow, CBF (ml/100 g per min)	177 ± 43
Hippocampal *N*-acetyl aspartate, NAA (mM)	6.62 ± 1.36
Respiration rate during NAA scan (breaths/min)	51 ± 3
Respiration rate during CBF scan (breaths/min)	52 ± 3

Values are expressed as mean ± standard deviation.
CBF, cerebral blood flow; Dahl-S, Dahl salt-sensitive; HR, heart rate; PWV, pulse wave velocity.

RESULTS

SBP, heart rate, aPWV, hippocampal CBF and NAA, collected in this cross-sectional study in 6 month-old Dahl-S rats, are presented in Table 1. The rats exhibited elevated SBP at this age. A symmetric correlation matrix of all parameters is presented in Table 2. The correlations above the diagonal (Table 2) were adjusted for FDR. Bivariate analysis revealed a positive borderline correlation between aPWV and SBP with a near-significant *P*-value of 0.06 and an R^2 value of 0.31 (Fig. 3). Notably, hippocampal CBF and aPWV demonstrated a strong negative Pearson correlation with a *P*-value <<0.001 and R^2 value of 0.79 (Fig. 4). Next, aPWV was negatively correlated with hippocampal NAA with a *P*-value of 0.03 and R^2 equal to 0.36 (Fig. 5). Finally, hippocampal NAA concentrations positively correlated with hippocampal CBF with a significant *P*-value of 0.03 and R^2 of 0.38 (Fig. 6). The Pearson correlation matrix of all individual simple regressions is presented in Table 2. As illustrated in this matrix, SBP did not correlate significantly with the brain MRI parameters. We also conducted multiple regression analysis for NAA and CBF models (Table S1,

TABLE 2. Correlation matrix of hemodynamic and MRI parameters in 6 month-old male Dahl-S rats

	SBP	aPWV	Hippo. CBF	Hippo. NAA
SBP	1	0.56	-0.42	-0.41
aPWV	0.56	1	-0.89	-0.60
Hippo. CBF	-0.42	-0.89	1	0.62
Hippo. NAA	-0.41	-0.60	0.62	1

Correlation coefficients for pairs of systemic hemodynamic and hippocampal parameters. Green boxes indicate correlations with $P < 0.05$. Yellow boxes correspond to those with $0.05 < P < 0.1$; $n = 12$. Color-coded boxes above the black diagonal refer to false discovery rate (FDR) adjusted *P* values. A strong negative correlation, which remained significant after FDR adjustment, was seen between aPWV and CBF.
aPWV, aortic pulse wave velocity; CBF, cerebral blood flow; hippo, hippocampal; Dahl-S, Dahl salt-sensitive; NAA, *N*-acetyl aspartate; SBP, systolic blood pressure.

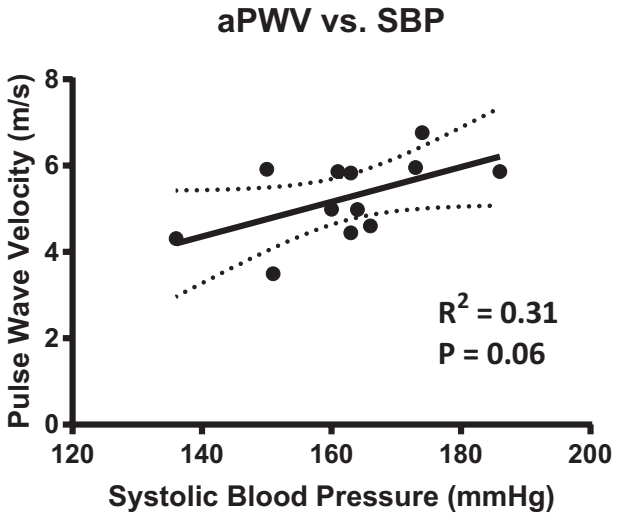

FIGURE 3 Regression of aortic pulse wave velocity (aPWV) with systolic blood pressure (SBP). aPWV, a marker of CAS, was near-significantly correlated with SBP, indicating that the latter might be numerically associated with vascular wall stiffening. $R^2 = 0.31$; $P = 0.06$; dotted lines, 95% confidence interval; $n = 12$. CAS, central arterial stiffness.

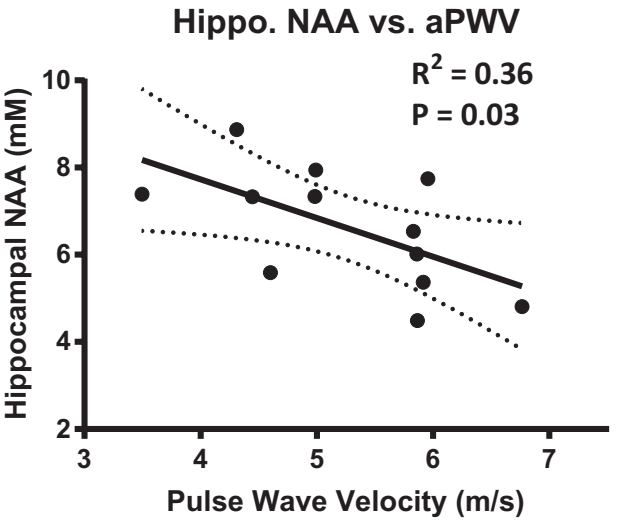

FIGURE 5 Regression of hippocampal *N*-acetyl aspartate (NAA) concentration and aortic pulse wave velocity (aPWV). A negative correlation between hippocampal NAA and aPWV suggests that CAS is associated with a loss of neuronal mass and viability. $R^2 = 0.36$; $P = 0.03$; dotted lines, 95% confidence interval; $n = 12$. CAS, central arterial stiffness.

Supplemental Digital Content, http://links.lww.com/HJH/B666 and Table S2, Supplemental Digital Content, http://links.lww.com/HJH/B666). Covariates included in multiple regression models were included based on the strongest bivariate associations with NAA or CBF. We considered the potential covariates of heart rate, body weight, SBP, and PWV in the model for hippocampal CBF. For the regression model for NAA, hippocampal CBF was also included (Tables S1, Supplemental Digital Content, http://links.lww.com/HJH/B666 and Table S2, Supplemental Digital Content, http://links.lww.com/HJH/B666). *P* values were near-significant (Table S1) or nonsignificant (Table S2) for all β coefficients corresponding to these covariates, resulting in the univariate models as described above.

DISCUSSION

Central arterial stiffness and systolic blood pressure

Numerous studies have linked hypertension with CAS. A common interpretation of relations between CAS and hypertension is that elevated BP increases pulsatile aortic wall stress [41]. Hasegawa *et al*. [42] found a direct relationship between aPWV and age in human subjects as well as significantly greater aPWV in hypertensive compared to age-matched normotensive subjects. Their analysis supported the conclusion that age was more significant than blood pressure in predicting aPWV. Similarly, Stratos *et al*. [43] found that aortic distensibility was lower in patients with arterial hypertension (SBP = 158 ± 17 mmHg) than in

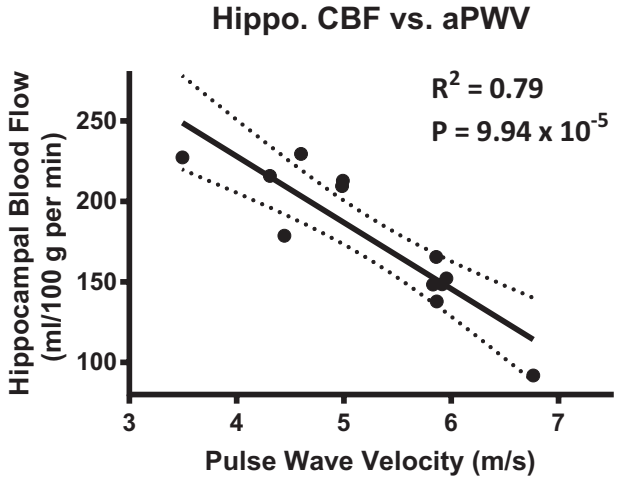

FIGURE 4 Regression of hippocampal cerebral blood flow (CBF) with aortic pulse wave velocity (aPWV). Higher aPWV was associated with lower hippocampal CBF, which suggests that CAS is associated with diminished cerebral perfusion. $R^2 = 0.79$; $P = 9.94 \times 10^{-5}$; dotted lines, 95% confidence interval; $n = 12$. CAS, central arterial stiffness.

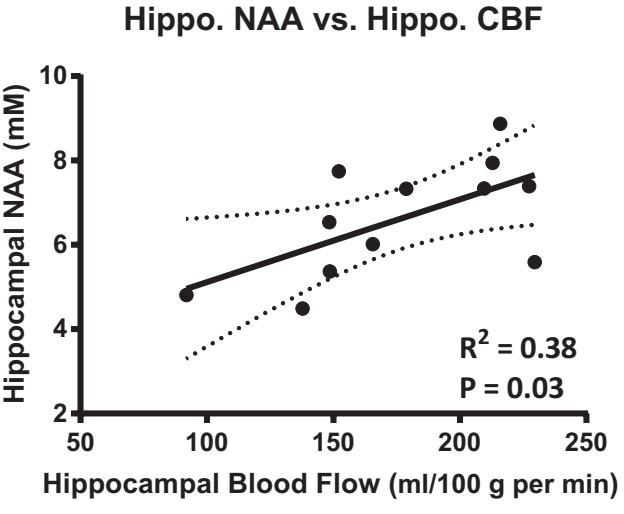

FIGURE 6 Regression of hippocampal *N*-acetyl aspartate (NAA) concentration and hippocampal cerebral blood flow (CBF). The positive correlation suggests that chronic cerebral hypoperfusion is associated with loss of neuronal mass and viability. $R^2 = 0.38$; $P = 0.03$; dotted lines, 95% confidence interval; $n = 12$.

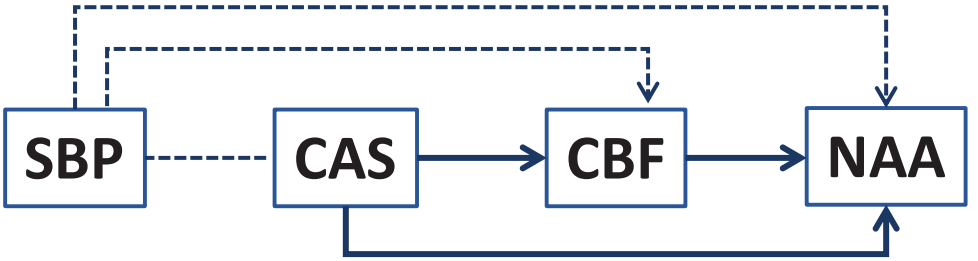

FIGURE 7 Schematic presentation of the associations between central arterial stiffness (CAS), measured as pulse wave velocity (PWV), systolic blood pressure (SBP), hippocampal *N*-acetyl aspartate (NAA) and hippocampal cerebral blood flow (CBF). Solid arrows indicate the detected associations; dotted lines indicate the proposed associations between parameters which will be further investigated.

normotensive subjects (SBP = 121 ± 8 mmHg). However, these results did not directly indicate whether the lower distensibility was due to structural differences or whether distensibility decreases as a function of pressure even in the absence of vessel wall changes. Thus, whether arterial stiffness is secondary to hypertension or vice versa, especially in elderly subjects, is unclear [12,44,45]. Nevertheless, several studies have shown that higher levels of CAS in normotensive individuals are associated with accelerated BP progression and increased risk for incident hypertension, defined as SBP ≥140 mmHg [46] or SBP ≥160 mmHg [47], during follow-up [46–49]. Moreover, it has been previously demonstrated that in men, BP and PWV increase with age at different rates, suggesting that while interrelated, changes in PWV and BP may be regulated by independent mechanisms [50].

An association between SBP and aPWV in the above clinical studies is in agreement with the finding in our cross-sectional study that SBP correlated positively with aPWV with borderline significance (Fig. 3). Beyond this, we sought to understand the influence of systemic hypertension and CAS on hippocampal CBF and NAA independent of age. We found that both markers of cerebral integrity exhibited a significant negative Pearson correlation with aPWV but not with SBP (Table 2). This indicates that there is a stronger association of brain MRI parameters with CAS than with SBP. We conclude that hypertension, which was defined as SBP >160 mmHg in the present study, is a possible consequence of increased CAS (Fig. 7), in agreement with the findings in previous clinical studies [46–50].

While both SBP and PWV measurements were taken at similar timepoints, they could not be measured simultaneously. In addition, SBP was measured in conscious animals to avoid the unnecessary stress of an additional period of anesthesia, while PWV required isoflurane anesthesia. This is likely to affect the quantitative relationship between these parameters, but, with all animals treated consistently, these measurements provide meaningful metrics for comparisons within groups. Nevertheless, the association of SBP with the other physiologic parameters studied, all measured under anesthesia, and their relationships with CAS, brain CBF and neuronal integrity, merits future study. Based on the results of the present study, we conclude that elevated aPWV may play a distinct mechanistic role in cerebral hypoperfusion and functional impairment. This is in agreement with previous clinical observations, which indicated that CAS was related to MRI-derived brain outcome measures, including reduced CBF, altered cerebral microcirculation, cerebral microbleeds and progression of white matter hyperintensities [6,11,25–27].

Measurements of systolic blood pressure, aortic pulse wave velocity, cerebral blood flow and *N*-acetyl aspartate

Our values for central arterial PWV, hippocampal CBF and NAA concentrations, obtained for 6 month-old Dahl-S rats (Table 1), are comparable to values found for Sprague-Dawley rats. Specifically, values for hippocampal NAA concentration (7.20 ± 2.65 mM, mean ± SD), hippocampal CBF (201 ± 37 ml/100 g/min, mean ± SD), and aPWV (5.23 ± 0.12 m/s, mean ± SD) were reported in 4 month-old Sprague-Dawley rats [51–53] matched in heart rate and estimated mean arterial pressure to Dahl-S rats in our present study (Table 1). Further, SBP and aPWV were higher in our 6 month-old adult Dahl-S rats than in 3 month-old young Dahl-S rats from our previously published paper (SBP: 162 ± 13 vs. 133 ± 9 mmHg; aPWV: 5.3 ± 0.9 vs. 2.6 ± 0.8 m/s, respectively; mean ± SD) [54]; this is consistent with the well-known phenomenon of an age-dependent increase in SBP and aPWV in human subjects [11,50,55–57].

Aortic pulse wave velocity and hippocampal blood flow

Previous studies have explored the relationship between central arterial PWV and CBF [11,25–27]. Kielstein *et al.* [27] established a relationship between increased CAS and decreased hippocampal CBF in human subjects secondary to administration of an endogenous nitric oxide synthase inhibitor, asymmetric dimethylarginine, with a greater effect seen in hypertensive than in normotensive subjects. Although this relationship was established with supraphysiological dimethylarginine blood levels, these results clearly demonstrate the effect of CAS on CBF. Additional studies have found that an increase in CAS was associated with a reduction in wave reflection at the interface between the carotid arteries and the aorta, with the increase in cerebral vessel pulsatility potentially resulting in microvascular and tissue damage [10,11]. This is consistent with the previous finding that greater CAS was associated with lower CBF in patients with dementia in comparison to age-matched normal controls [23].

In the present work, we observed a strong, negative Pearson correlation between hippocampal CBF and aPWV

in 6 month-old male Dahl-S rats (Fig. 4). Specifically, the observation of lower levels of hippocampal CBF in animals with greater aPWV suggests that CAS plays a significant role in diminishing hippocampal perfusion, potentially through the impedance-matching mechanism mentioned earlier [10,11,25,26]. This proposed mechanism should be further evaluated in longitudinal studies.

Hippocampal blood flow and neuronal density

Previous work in a murine model of malaria demonstrated that reduced CBF was associated with lower levels of the ratio NAA/Cr [58]; this was attributed to decreased oxygen availability for oxidative phosphorylation. We found a similar relation between hippocampal NAA and CBF in our study on adult Dahl-S rats (Fig. 6). However, this correlation was weaker than that between hippocampal CBF and aPWV (Fig. 4). This is consistent with overall adequacy of substrate delivery in our Dahl-S rats, but also suggests that further increases in CAS, with concomitant decreases in CBF, may have a negative impact on neuronal viability. Our present observation is supported by data from a study of experimental stroke in rats, which demonstrated a threshold in CBF of 62–94 ml/100 g per min, below which marked neuronal damage occurs [59].

Aortic pulse wave velocity and hippocampal neuronal density

In our work, the simultaneous occurrence of similar, though opposite correlations of hippocampal NAA concentration with aPWV (Fig. 5) and hippocampal NAA with hippocampal CBF (Fig. 6) together with the much stronger correlation between CBF and aPWV (Fig. 4) suggest that the NAA correlations are not independent of one another. Indeed, an indirect association of NAA concentration with aPWV is consistent with the proposed mechanism linking CAS with reduced CBF (Fig. 7).

Potential consequences for cognitive function

Hypertension is associated with a greater incidence of cerebrovascular disease and dementia with aging [1–5,9]. Further, in clinical studies, BP management resulted in improved cognitive function in patients with vascular dementia [60,61]. Cerebral NAA concentration is known to be directly associated with cognitive function [62,63]. We focused on the hippocampal parameters in our present study, given their direct association with memory manifestations in cognitive impairment and dementia [64,65]. In our study, SBP did not correlate significantly with hippocampal CBF or NAA concentration and we found that aPWV was more closely correlated with CBF and NAA than was SBP (Table 2). These observations suggest that the connection between hypertension and cognitive deficits may be indirect and very likely mediated by CAS and cerebral hypoperfusion in the Dahl-S model.

Limitations

The cross-sectional nature of our study in adult, 6 month-old, male Dahl-S rats represents a limitation in establishing causal relationships between the measured outcomes, including between CAS and cerebrovascular changes. Further, CBF values may be particularly susceptible to the acute physiologic status of the animal, although we attempted to maintain strict consistency in animal handling [66]. In addition, CBF measurements with MRI are notoriously difficult; in our experiment, we were able to operate at a high field strength and use advanced filtering techniques to increase the reliability of the results. Likewise, the localized spectra from which NAA concentrations are derived are necessary of limited SNR; we implemented an optimized procedure including localized shimming within the hippocampus to maximize sensitivity. An additional limitation of this study is the fact that SBP was measured in conscious animals to avoid unnecessary additional physiologic stress, while PWV and brain MRI measurements were performed under isoflurane anesthesia; this has been discussed extensively above. In addition, these parameters cannot be collected simultaneously due to constraints imposed by the MRI system.

In conclusion, in the Dahl-S rat model of age-associated vascular dementia, we observed a significant association between higher aPWV, a marker for CAS, and lower hippocampal perfusion and lower NAA, a marker of neuronal viability. Combined with the dependence of hippocampal neuronal mass and viability on adequate perfusion, our findings suggest a potential mechanistic link between age-associated CAS, deficits in the cerebral circulation, loss of neuronal density and cognitive impairment. This may support CAS as a potential therapeutic target for the prevention and treatment of age-associated neurodegenerative diseases.

PERSPECTIVES

Our study demonstrates the connection of central arterial stiffness and cerebral hypoperfusion and neurodegeneration in the Dahl-S rat model of age-associated hypertension, which occurs in the absence of high salt intake. Our study suggests that in this model, CAS significantly enhances the pulsatility of blood flow, resulting in cerebral microvascular damage and reduced cerebral blood flow to the brain cells, thereby contributing to neurodegeneration.

ACKNOWLEDGEMENTS

S.O.A. and R.C.F. conducted experiments and acquired data. S.O.A., R.C.F., Y.N.G., D.C., C.H.M. and M.B. analyzed and interpreted the data. S.O.A., E.G.L., R.G.S., O.V.F. and K.W.F. participated in conceptual development, experimental design, and data interpretation. S.O.A., E.G.L., R.G.S., O.V.F. and K.W.F. wrote, edited and revised the article. The authors highly appreciate the input of Dr Natalia Petrashevskaya in this work, who participated in the measurement of pulse wave velocity and in the data analysis and interpretation.

Presented in part at the Alzheimer's Association International Conference 2019.

Sources of Funding: This work was supported by the Intramural Research Program, National Institute on Aging, National Institutes of Health, USA.

Conflicts of interest

There are no conflicts of interest.

REFERENCES

1. Launer LJ, Masaki K, Petrovitch H, Foley D, Havlik RJ. The association between midlife blood pressure levels and late-life cognitive function. The Honolulu-Asia Aging Study. *JAMA* 1995; 274:1846–1851.
2. Qiu C, Winblad B, Fratiglioni L. The age-dependent relation of blood pressure to cognitive function and dementia. *Lancet Neurol* 2005; 4:487–499.
3. Girouard H, Iadecola C. Neurovascular coupling in the normal brain and in hypertension, stroke, and Alzheimer disease. *J Appl Physiol* 2006; 100:328–335.
4. de la Torre JC. Alzheimer disease as a vascular disorder: nosological evidence. *Stroke* 2002; 33:1152–1162.
5. Farkas E, Luiten PG. Cerebral microvascular pathology in aging and Alzheimer's disease. *Prog Neurobiol* 2001; 64:575–611.
6. Gorelick PB, Scuteri A, Black SE, Decarli C, Greenberg SM, Iadecola C, *et al*. Vascular contributions to cognitive impairment and dementia: a statement for healthcare professionals from the American Heart Association/American Stroke Association. *Stroke* 2011; 42:2672–2713.
7. de la Torre JC. Cerebral hemodynamics and vascular risk factors: setting the stage for Alzheimer's disease. *J Alzheimers Dis* 2012; 32:553–567.
8. de la Torre JC. Cardiovascular risk factors promote brain hypoperfusion leading to cognitive decline and dementia. *Cardiovasc Psychiatry Neurol* 2012; 2012:367516.
9. Iadecola C, Davisson RL. Hypertension and cerebrovascular dysfunction. *Cell Metab* 2008; 7:476–484.
10. Mitchell GF. Effects of central arterial aging on the structure and function of the peripheral vasculature: implications for end-organ damage. *J Appl Physiol* 2008; 105:1652–1660.
11. Mitchell GF, van Buchem MA, Sigurdsson S, Gotal JD, Jonsdottir MK, Kjartansson O, *et al*. Arterial stiffness, pressure and flow pulsatility and brain structure and function: the Age, Gene/Enivronment Susceptibility—Reykjavik study. *Brain* 2011; 134 (Pt 11):3398–3407.
12. Safar ME, Asmar R, Benetos A, Blacher J, Boutouyrie P, Lacolley P, *et al*. Interaction between hypertension and arterial stiffness. *Hypertension* 2018; 72:796–805.
13. Thompson B, Towler DA. Arterial calcification and bone physiology: role of the bone-vascular axis. *Nat Rev Endocrinol* 2012; 8:529–543.
14. Gaballa MA, Jacob CT, Raya TE, Liu J, Simon B, Goldman S. Large artery remodeling during aging: biaxial passive and active stiffness. *Hypertension* 1998; 32:437–443.
15. Fleenor BS, Marshall KD, Durrant JR, Lesniewski LA, Seals DR. Arterial stiffening with ageing is associated with transforming growth factor-beta1-related changes in adventitial collagen: reversal by aerobic exercise. *J Physiol* 2010; 588 (Pt 20):3971–3982.
16. Hays TT, Ma B, Zhou N, Stoll S, Pearce WJ, Qiu H, *et al*. Vascular smooth muscle cells direct extracellular dysregulation in aortic stiffening of hypertensive rats. *Aging Cell* 2018; 17:e12748; doi: 10.1111/acel.12748.
17. Fleenor BS. Large elastic artery stiffness with aging: novel translational mechanisms and interventions. *Aging Dis* 2013; 4:76–83.
18. Grigorova YN, Wei W, Petrashevskaya N, Zernetkina V, Juhasz O, Fenner R, *et al*. Dietary sodium restriction reduces arterial stiffness, vascular TGF-beta-dependent fibrosis and marinobufagenin in young normotensive rats. *Int J Mol Sci* 2018; 19:3168.
19. Sehgel NL, Sun Z, Hong Z, Hunter WC, Hill MA, Vatner DE, *et al*. Augmented vascular smooth muscle cell stiffness and adhesion when hypertension is superimposed on aging. *Hypertension* 2015; 65:370–377.
20. AlGhatrif M, Wang M, Fedorova OV, Bagrov AY, Lakatta EG. The pressure of aging. *Med Clin North Am* 2017; 101:81–101.
21. Pereira T, Correia C, Cardoso J. Novel methods for pulse wave velocity measurement. *J Med Biol Eng* 2015; 35:555–565.
22. McEniery CM, Wilkinson IB, Avolio AP. Age, hypertension and arterial function. *Clin Exp Pharmacol Physiol* 2007; 34:665–671.
23. Wilkinson IB, MacCallum H, Cockcroft JR, Webb DJ. Inhibition of basal nitric oxide synthesis increases aortic augmentation index and pulse wave velocity in vivo. *Br J Clin Pharmacol* 2002; 53:189–192.
24. Magistretti P, Pellerin L. Cellular mechanisms of brain energy metabolism. Relevance to functional brain imaging and to neurodegenerative disorders. *Ann N Y Acad Sci* 1996; 777:380–387.
25. Jefferson AL, Cambronero FE, Liu D, Moore EE, Neal JE, Terry JG, *et al*. Higher aortic stiffness is related to lower cerebral blood flow and preserved cerebrovascular reactivity in older adults. *Circulation* 2018; 138:1951–1962.
26. Poels MMF, Zaccai K, Verwoert GC, Vernooij MW, Hofman A, van der Lugt A, *et al*. Arterial stiffness and cerebral small vessel disease. *Stroke* 2012; 43:2637–2642.
27. Kielstein JT, Donnerstag F, Gasper S, Menne J, Kielstein A, Martens-Lobenhoffer J, *et al*. ADMA increases arterial stiffness and decreases cerebral blood flow in humans. *Stroke* 2006; 37:2024–2029.
28. Rosso IM, Crowley DJ, Silveri MM, Rauch SL, Jensen JE. Hippocampus glutamate and *N*-acetyl aspartate markers of excitotoxic neuronal compromise in posttraumatic stress disorder. *Neuropsychopharmacology* 2017; 42:1698–1705.
29. Clark JB. *N*-Acetyl aspartate: a marker for neuronal loss or mitochondrial dysfunction. *Dev Neurosci* 1998; 20:271–276.
30. van der Knaap MS, van der Grond J, Luyten PR, den Hollander JA, Nauta JJ, Valk J, *et al*. ^{1}H and ^{31}P magnetic resonance spectroscopy of the brain in degenerative cerebral disorders. *Ann Neurol* 1992; 31:202–211.
31. Moffett JR, Ross B, Arun P, Madhavarao CN, Namboodiri AMA. N-Acetylaspartate in the CNS: from neurodiagnostics to neurobiology. *Prog Neurobiol* 2007; 81:89–131.
32. Shiino A, Matsuda M, Morikawa S, Inubushi T, Akiguchi I, Handa J. Proton magnetic resonance spectroscopy with dementia. *Surg Neurol* 1993; 39:143–147.
33. Zicha J, Dobesova Z, Vokurkova M, Rauchova H, Hojna S, Kadlecova M, *et al*. Age-dependent salt hypertension in Dahl rats: fifty years of research. *Physiol Res* 2012; 61 (Suppl 1):S35–S87.
34. Fedorova OV, Grigorova YN, Hagood M, Long J, McDevitt R, McPherson R, *et al*. Cognitive impairment is associated with premature arterial stiffening, aortic wall fibrosis and increased blood pressure: a novel rat model of age-dependent vascular dementia. *Alzheimers Dementia* 2018; 18:1149–1150.
35. Wilde E, Aubdool AA, Thakore P, Baldissera L Jr, Alawi KM, Keeble J, *et al*. Tail-cuff technique and its influence on central blood pressure in the mouse. *J Am Heart Assoc* 2017; 6:e005204.
36. Ahmet I, Tae HJ, Brines M, Cerami A, Lakatta EG, Talan MI, *et al*. Chronic administration of small nonerythropoietic peptide sequence of erythropoietin effectively ameliorates the progression of postmyocardial infarction-dilated cardiomyopathy. *J Pharmacol Exp Ther* 2013; 345:446–456.
37. Provencher SW. Estimation of metabolite concentrations from localized in vivo proton NMR spectra. *Magn Reson Med* 1993; 30:672–679.
38. Bouhrara M, Lee DY, Rejimon AC, Bergeron CM, Spencer RG. Spatially adaptive unsupervised multispectral nonlocal filtering for improved cerebral blood flow mapping using arterial spin labeling magnetic resonance imaging. *J Neurosci Methods* 2018; 309:121–131.
39. Barbier EL, Lawrence KS, Grillon E, Koretsky AP, Decorps M. A model of blood-brain barrier permeability to water: accounting for blood inflow and longitudinal relaxation effects. *Magn Reson Med* 2002; 47:1100–1109.
40. Lu H, Leoni R, Silva AC, Stein EA, Yang Y. High-field continuous arterial spin labeling with long labeling duration: reduced confounds from blood transit time and postlabeling delay. *Magn Reson Med* 2010; 64:1557–1566.
41. Oparil S, Zaman MA, Calhoun DA. Pathogenesis of hypertension. *Ann Intern Med* 2003; 139:761–776.
42. Hasegawa M, Nagao K, Kinoshita Y, Rodbard D, Asahina A. Increased pulse wave velocity and shortened pulse wave transmission time in hypertension and aging. *Cardiology* 1997; 88:147–151.
43. Stratos C, Stefanadis C, Kallikazaros I, Boudoulas H, Toutouzas P. Ascending aorta distensibility abnormalities in hypertensive patients and response to nifedipine administration. *Am J Med* 1992; 93:505–512.
44. Mitchell GF. Arterial stiffness and hypertension: chicken or egg? *Hypertension* 2014; 64:210–214.
45. Kaess BM, Rong J, Larson MG, Hamburg NM, Vita JA, Levy D, *et al*. Aortic stiffness, blood pressure progression, and incident hypertension. *JAMA* 2012; 308:875–881.
46. Najjar SS, Scuteri A, Shetty V, Wright JG, Muller DC, Fleg JL, *et al*. Pulse wave velocity is an independent predictor of the longitudinal increase in systolic blood pressure and of incident hypertension in the Baltimore Longitudinal Study of Aging. *J Am Coll Cardiol* 2008; 51:1377–1383.
47. Dernellis J, Panaretou M. Aortic stiffness is an independent predictor of progression to hypertension in nonhypertensive subjects. *Hypertension* 2005; 45:426–431.

48. Liao D, Arnett DK, Tyroler HA, Riley WA, Chambless LE, Szklo M, *et al.* Arterial stiffness and the development of hypertension. The ARIC study. *Hypertension* 1999; 34:201–206.
49. Takase H, Dohi Y, Toriyama T, Okado T, Tanaka S, Sonoda H, *et al.* Brachial-ankle pulse wave velocity predicts increase in blood pressure and onset of hypertension. *Am J Hypertens* 2011; 24:667–673.
50. Scuteri A, Morrell CH, Orru M, Strait JB, Tarasov KV, Ferreli LA, *et al.* Longitudinal perspective on the conundrum of central arterial stiffness, blood pressure, and aging. *Hypertension* 2014; 64:1219–1227.
51. Poland RE, Cloak C, Lutchmansingh PJ, McCracken JT, Chang L, Ernst T, *et al.* Brain N-acetyl aspartate concentrations measured by 1H MRS are reduced in adult male rats subjected to perinatal stress: preliminary observations and hypothetical implications for neurodevelopmental disorders. *J Psychiatric Res* 1999; 33:41–51.
52. Tan I, Butlin M, Liu YY, Ng K, Avolio AP. Heart rate dependence of aortic pulse wave velocity at different arterial pressures in rats. *Hypertension* 2012; 60:528–533.
53. Drabek T, Foley LM, Janata A, Stezoski J, Hitchens TK, Manole MD, *et al.* Global and regional differences in cerebral blood flow after asphyxial versus ventricular fibrillation cardiac arrest in rats using ASL-MRI. *Resuscitation* 2014; 85:964–971.
54. Zhang Y, Wei W, Shilova V, Petrashevskaya NN, Zernetkina VI, Grigorova YN, *et al.* Monoclonal antibody to marinobufagenin down-regulates TGFbeta profibrotic signaling in left ventricle and kidney and reduces tissue remodeling in salt-sensitive hypertension. *J Am Heart Assoc* 2019; 8:e012138.
55. Sutton-Tyrrell K, Najjar SS, Boudreau RM, Venkitachalam L, Kupelian V, Simonsick EM, *et al.* Elevated aortic pulse wave velocity, a marker of arterial stiffness, predicts cardiovascular events in well functioning older adults. *Circulation* 2005; 111:3384–3390.
56. Kotchen JM, McKean HE, Kotchen TA. Blood pressure trends with aging. *Hypertension* 1982; 4:128–134.
57. Oberdier MT, Morrell CH, Lakatta EG, Ferrucci L, AlGhatrif M. Subclinical longitudinal change in ankle-brachial index with aging in a community-dwelling population is associated with central arterial stiffening. *J Am Heart Assoc* 2019; 8:e011650; doi: 10.1161/jaha.118.011650.
58. Kennan RP, Machado FS, Lee SC, Desruisseaux MS, Wittner M, Tsuji M, *et al.* Reduced cerebral blood flow and *N*-acetyl aspartate in a murine model of cerebral malaria. *Parasitol Res* 2005; 96:302–307.
59. Nagasawa H, Kogure K. Correlation between cerebral blood flow and histologic changes in a new rat model of middle cerebral artery occlusion. *Stroke* 1989; 20:1037–1043.
60. Launer LJ. Blood pressure control as an intervention to prevent dementia. *Lancet Neurol* 2019; 18:906–908.
61. Ding J, Davis-Plourde KL, Sedaghat S, Tully PJ, Wang W, Phillips C, *et al.* Antihypertensive medications and risk for incident dementia and Alzheimer's disease: a meta-analysis of individual participant data from prospective cohort studies. *Lancet Neurol* 2020; 19:61–70.
62. Baslow MH. *N*-Acetylaspartate in the vertebrate brain: metabolism and function. *Neurochem Res* 2003; 28:941–953.
63. Dicke U, Roth G. Neuronal factors determining high intelligence. *Philos Trans R Soc Lond B Biol Sci* 2016; 371:20150180.
64. Costafreda SG, Dinov ID, Tu Z, Shi Y, Liu C-Y, Kloszewska I, *et al.* Automated hippocampal shape analysis predicts the onset of dementia in mild cognitive impairment. *Neuroimage* 2011; 56:212–219.
65. La Joie R, Perrotin A, de La Sayette V, Egret S, Doeuvre L, Belliard S, *et al.* Hippocampal subfield volumetry in mild cognitive impairment, Alzheimer's disease and semantic dementia. *Neuroimage Clin* 2013; 3:155–162.
66. Kato K, Wakai J, Ozawa K, Sekiguchi M, Katahira K. Different sensitivity to the suppressive effects of isoflurane anesthesia on cardiorespiratory function in SHR/Izm, WKY/Izm, and Crl: CD (SD) rats. *Exp Anim* 2016; 65:393–402.